Small molecule targeting Cdc42–intersectin interaction disrupts Golgi organization and suppresses cell motility

Amy Friesland[a,1], Yaxue Zhao[b,c,1], Yan-Hua Chen[a,d], Lie Wang[b], Huchen Zhou[b,c,2], and Qun Lu[a,d,e,2]

[a]Department of Anatomy and Cell Biology, Brody School of Medicine, East Carolina University, Greenville, NC 27834; [b]School of Pharmacy, Shanghai Jiao Tong University, Shanghai 200240, China; [c]State Key Laboratory of Microbial Metabolism, Shanghai Jiao Tong University, Shanghai 200240, China; [d]Leo Jenkins Cancer Center, Brody School of Medicine, East Carolina University, Greenville, NC 27834; and [e]The Harriet and John Wooten Laboratory for Alzheimer's Disease and Neurodegenerative Diseases Research, Brody School of Medicine, East Carolina University, Greenville, NC 27834

Edited by Alan R. Fersht, Medical Research Council Laboratory of Molecular Biology, Cambridge, United Kingdom, and approved November 27, 2012 (received for review October 11, 2011)

Signaling through the Rho family of small GTPases has been intensely investigated for its crucial roles in a wide variety of human diseases. Although RhoA and Rac1 signaling pathways are frequently exploited with the aid of effective small molecule modulators, studies of the Cdc42 subclass have lagged because of a lack of such means. We have applied high-throughput *in silico* screening and identified compounds that are able to fit into the surface groove of Cdc42, which is critical for guanine nucleotide exchange factor binding. Based on the interaction between Cdc42 and intersectin (ITSN), a specific Cdc42 guanine nucleotide exchange factor, we discovered compounds that rendered ITSN-like interactions in the binding pocket. By using in vitro binding and imaging as well as biochemical and cell-based assays, we demonstrated that ZCL278 has emerged as a selective Cdc42 small molecule modulator that directly binds to Cdc42 and inhibits its functions. In Swiss 3T3 fibroblast cultures, ZCL278 abolished microspike formation and disrupted GM130-docked Golgi structures, two of the most prominent Cdc42-mediated subcellular events. ZCL278 reduces the perinuclear accumulation of active Cdc42 in contrast to NSC23766, a selective Rac inhibitor. ZCL278 suppresses Cdc42-mediated neuronal branching and growth cone dynamics as well as actin-based motility and migration in a metastatic prostate cancer cell line (i.e., PC-3) without disrupting cell viability. Thus, ZCL278 is a small molecule that specifically targets Cdc42–ITSN interaction and inhibits Cdc42-mediated cellular processes, thus providing a powerful tool for research of Cdc42 subclass of Rho GTPases in human pathogenesis, such as those of cancer and neurological disorders.

Cdc42 inhibitor | computer-assisted virtual screening | protein–protein interaction | cytoskeleton | protein trafficking

Cdc42, a member of the Rho GTPase family of low molecular weight G proteins, is an important regulator of many biological processes. First identified by its involvement in the establishment of polarity in *Saccharomyces cerevisiae*, Cdc42 has since been shown to play key roles in cytoskeletal organization, vesicular trafficking, cell cycle control, and transcription (1–3). As with most GTPases, transduction of signals occurs through the exchange of GDP for GTP, thus activating Cdc42 (4). The cycling between nucleotide-dependent conformation states of Rho family GTPases is supported by three regulatory proteins: guanine nucleotide exchange factors (GEFs), GTPase activation proteins (GAPs), and guanine nucleotide dissociation inhibitors (GDIs). GEFs facilitate activation of the GTPase by catalyzing the exchange of bound GDP for GTP, whereas GAPs promote the GDP-bound conformation (5, 6). Additional negative regulation occurs through GDIs, which sequester Rho proteins in the cytoplasm and prevent nucleotide exchange (7).

Recent studies have implicated aberrant Cdc42 activity in a variety of human pathologic processes, including cancer and neurodegeneration (3, 8). Interestingly, no mutations in the Cdc42 gene attributing to human cancer have been identified (9). Abnormal phenotypes appear to be caused by deregulation or overexpression of Cdc42 in an apparent tissue- and microenvironment-dependent fashion (3). Cdc42 has been attributed to several aspects of cancer, including cellular transformation (10) and metastasis (11, 12). As a key regulator of neurite morphogenesis, Cdc42 has also been shown to be crucial for normal brain development, as conditional Cdc42 KO mice do not survive birth and show gross brain abnormalities (8, 13).

However, among the three classical Rho subfamilies, studies of Cdc42 signaling lag behind those of RhoA and Rac1. This is partly because of the more rapid activation–inactivation cycles of Cdc42 in the cells and the lack of selective small-molecule tools to aid in capturing this process directly. In the present study, we have used computer-assisted virtual screening to identify compounds that are able to fit into the surface groove of Cdc42, which is critical for GEF binding. Based on Cdc42's interaction with intersectin (ITSN), a specific Cdc42 GEF, chemical compounds that rendered ITSN-like interactions in the binding pocket were preferentially selected for further investigation (14–16). We have now determined ZCL278 as a potent, cell-permeable Cdc42-specific small-molecule inhibitor that suppresses actin-based cellular functions, including Golgi organization and cell motility.

Results

Virtual Screening for Cdc42 Inhibitors. Analysis of the 3D structure of Cdc42–ITSN complex (Protein Data Bank ID code 1KI1) revealed a main binding region between Cdc42 and ITSN (16). Residues Gln1380 and Arg1384 of ITSN were observed to form hydrogen bonds with Asn39 and Phe37 of Cdc42, respectively. Two clusters of hydrophobic interactions were found between Leu1376, Met1379, and Thr1383 of ITSN and Phe56, Tyr64, Leu67, and Leu70 of Cdc42. To screen for Cdc42 inhibitors, the putative binding pocket on Cdc42 was created within 7 Å of the center of the aforementioned ITSN residues that interact with Cdc42. The binding pocket consists of 16 Cdc42 residues including Thr35, Val36, Asn39, Phe56, and Asp57 (Fig. 1*A*). The 197,000 compounds from the Specs Chemistry Database (www.specs.net) were screened by using high-throughput virtual screening and standard precision docking sequentially. The top-ranked 100 molecules were subjected to manual inspection according to the following criteria: ITSN-like binding posture and occupation for the Leu1376, Gln1380, Arg1384, Met1379, and Thr1383 residue space of ITSN should be observed; at least three hydrogen bonds should be formed; a conserved hydrogen bond with Asn39 or Phe37 of Cdc42 should exist; and diversity of scaffolds should be considered. A selection of 30 compounds was eventually tested on their ability to disrupt against Cdc42 activity and/or functions.

Author contributions: Y.-H.C., H.Z., and Q.L. designed research; A.F., Y.Z., L.W., and Q.L. performed research; Y.-H.C. contributed new reagents/analytic tools; A.F., Y.Z., Y.-H.C., H.Z., and Q.L. analyzed data; and A.F., Y.Z., Y.-H.C., H.Z., and Q.L. wrote the paper.

The authors declare no conflict of interest.

This article is a PNAS Direct Submission.

[1]A.F. and Y.Z. contributed equally to this work.

[2]To whom correspondence may be addressed. E-mail: luq@ecu.edu or hczhou@sjtu.edu.cn.

This article contains supporting information online at www.pnas.org/lookup/suppl/doi:10.1073/pnas.1116051110/-/DCSupplemental.

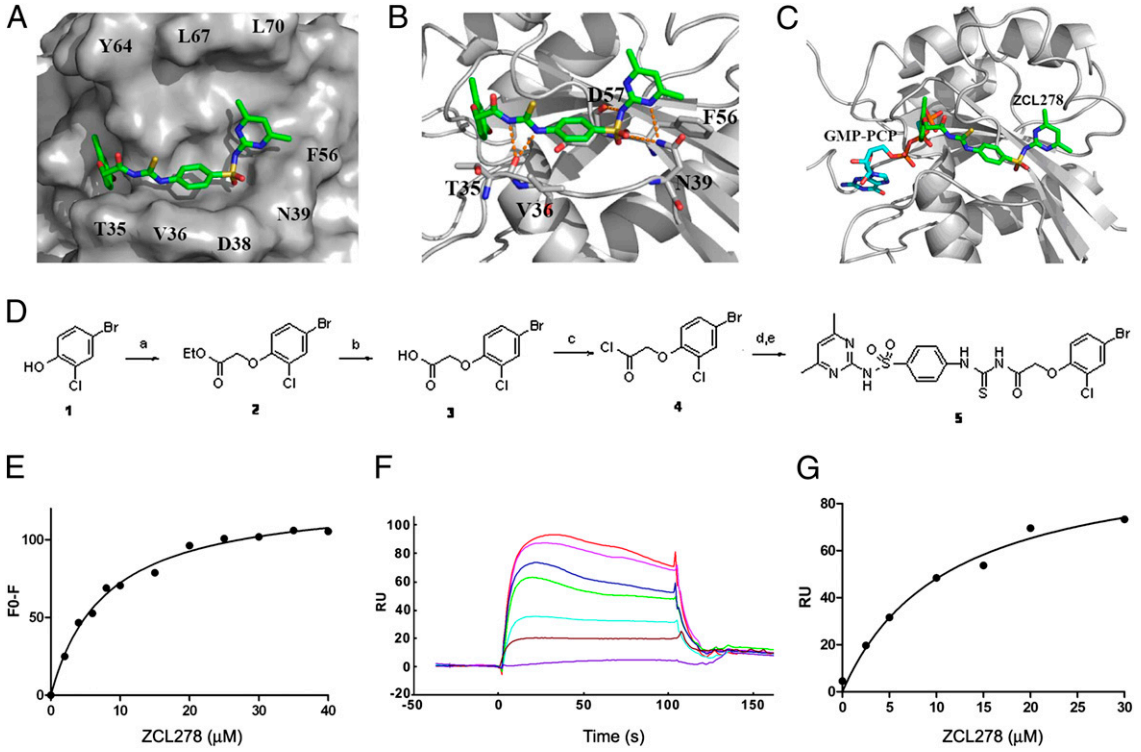

Fig. 1. Identification of ZCL compounds targeting Cdc42–ITSN interaction. (*A*) Docked pose of ZCL278 in the Cdc42 binding pocket: protein is shown as gray surface; ligand is shown as green sticks. (*B*) Proposed interactions between ZCL278 and Cdc42 residues: ZCL278 is shown as green sticks; Cdc42 is shown as gray cartoon; residues of Cdc42 are shown as gray sticks; hydrogen bonds are represented as orange dashed lines. (*C*) Superposition of GMP-PCP (Protein Data Bank ID code 2QRZ) and the docked Cdc42–ZCL278 complex. Cdc42 is indicated by gray cartoon; ZCL278 by green sticks; and GMP-PCP by cyan sticks. (*D*) Synthesis of ZCL278. Reagents and conditions are as follows: *a*, Ethyl 2-bromoacetate, K_2CO_3, DMF, 70 °C; *b*, NaOH, dioxane/H_2O; *c*, $SOCl_2$, DMF, reflux; *d*, NaSCN, acetone, 0 °C to room temperature; and *e*, 4-amino-N-(4,6-dimethylpyrimidin-2-yl) benzenesulfonamide, 0 °C to room temperature. Note: GMP-PCP is GTP analogue guanylyl-β, γ-methylene-diphosphonate (i.e., the presumed signaling-active state). (*E*) Fluorescence titration of Cdc42 with compound ZCL278. Fluorescence emission at 350 nm was monitored (K_d = 6.4 μM). (*F*) SPR measurement of Cdc42–ZCL278 interaction. (*G*) SPR determined at a K_d of 11.4 μM for Cdc42-ZCL278 affinity.

Computed Binding Mode of ZCL278 in Cdc42. As shown in Fig. 1*A*, one small molecule, termed ZCL278, bound to a well formed Cdc42 pocket lined by residues Thr35, Val36, Asp38, Asn39, Phe56, Tyr64, Leu67, and Leu70. The docked pose suggests extensive favorable interactions between ZCL278 and Cdc42 residues. Five hydrogen bonds involving residues Thr35, Asn39, and Asp57, as well as hydrophobic interactions associated with residues Val36 and Phe56, were observed (Fig. 1*B*). The bromophenyl ring was inserted into the adjacent GTP/GDP binding pocket. The computed binding mode suggests that ZCL278 should be able to disrupt the Cdc42–ITSN interaction as well as GTP/GDP binding (Fig. 1*C*). Indeed, the competition between GTP and ZCL278 to influence Cdc42 GTPase activity was confirmed by using p50RhoGAP or Cdc42GAP assay (Fig. S1). Our docking studies suggest that increasing GTP addition can compete with preloaded ZCL278 on Cdc42 and increase GTP hydrolysis by purified recombinant Cdc42 protein in vitro. Thus, local GTP/GDP should have impact on the effective doses of ZCL278 in the cells.

Synthesis of Cdc42 Inhibitor ZCL278. To confirm the screening hits and provide high-purity samples for biological exploitation, ZCL278 was synthesized, purified, and characterized. As illustrated in a scheme (Fig. 1*D*), after compound 2 (*SI Materials and Methods*) was prepared from 4-bromo-2-chlorophenol and ethyl 2-bromoacetate in the presence of potassium carbonate, it was hydrolyzed in the alkali condition to provide the acid compound 3 (*SI Materials and Methods*). Treatment of compound 3 with refluxing thionyl chloride with dimethyl formamide (DMF) as a catalyst gave acyl chloride (compound 4; *SI Materials and Methods*), which was converted to 4-(3-(2-(4-bromo-2-chloro-phenoxy)-acetyl)-thioureido)-N-(4,6-dimethyl-pyrimidin-2-yl)-benzenesulfonamide (compound 5; ZCL278) after treatment with sodium thiocyanate, followed by reaction with 4-amino-N-(4,6-dimethylpyrimidin-2-yl) benzene-sulfonamide.

Direct Binding of ZCL278 and Cdc42 Demonstrated by Fluorescence Titration and Surface Plasmon Resonance. We assessed the binding affinity of ZCL278 and Cdc42 by using two independent biophysical methods. First, fluorescence titration of purified Cdc42 by ZCL278 was carried out by monitoring the change of fluorescence intensity of a tryptophan residue on Cdc42 upon ZCL278 binding. As ZCL278 has a weak absorption peak at 310 nm, to avoid any experimental error that might result from potential fluorescence quenching by ZCL278, the fluorescence emission of Cdc42 was monitored at 350 nm, at which ZCL278 has a negligible absorption. Thus, a K_d value of 6.4 μM was obtained (Fig. 1*E*). To further demonstrate the direct interaction between ZCL278 and Cdc42, a surface plasmon resonance (SPR) experiment was performed by covalently immobilizing purified Cdc42 onto CM5 chips and varying ZCL278 concentration. The SPR response was observed to increase along with elevated ZCL278 concentrations, and eventually gave a K_d of 11.4 μM (Fig. 1 *F* and *G*). To support the K_d measured in our system, the solubility of ZCL278 was determined to be 181 μM and was greater than the concentrations used in all experiments in this study (*SI Materials and Methods*). The experimental pK_a values of ZCL278 were determined to be 3.48 ± 0.04, 6.61 ± 0.02, and 7.45 ± 0.01 (*SI Materials and Methods*). The pK_a value of 3.48 is associated to pyrimidine nitrogen that should stay in a neutral form at pH 7.4. The NH groups corresponding to pK_a values of 6.61 and 7.45 should be partially deprotonated and give

a population of charged species in solution. These species in solution may have modifying effects on membrane transport and binding to Cdc42.

ZCL278 Inhibits Cdc42-Mediated Microspike Formation. We assessed the 30 selected ZCL compounds for their ability to inhibit Cdc42-mediated microspike/filopodia formation in serum-starved Swiss 3T3 fibroblasts. Actin-based microspikes/filopodia are characteristic of Cdc42 activity in cultured fibroblastic cells (17, 18). As shown in Fig. 2*A*, DMSO-treated (Fig. 2*A*, control) cells have few microspikes along their perimeter (Fig. 2*A*, arrows), as well as the characteristic presence of RhoA-mediated stress fibers (Fig. 2*A*, asterisk). When arrested fibroblasts were briefly stimulated with 1 U/mL of a commercial Cdc42 activator, a dramatic increase in microspike number and decrease in stress fibers occurred (Fig. 2*A*, activator). Compound ZCL278 was applied at 50 μM for 15 min or 1 h and then stimulated with the Cdc42 activator for 2 min. After 15 min incubation, the cell periphery of ZCL278-treated cells resembles that of control cells, with few microspikes (Fig. 2*A*, ZCL278). Following 1 h of ZCL278 treatment and Cdc42 stimulation, there is obvious inhibition of microspike formation (Fig. 2*A*, activator + ZCL278) compared with cells treated with only the activator (Fig. 2*A*, activator). ZCL197 and ZCL279, two other compounds with favorable predicted binding to Cdc42, failed to inhibit microspike formation (Fig. 2*A*, activator + ZCL197), or induced branched cellular processes resembling RhoA suppression (Fig. 2*A*, activator + ZCL279). Therefore, ZCL278, but not ZCL197 or ZCL279, inhibits Cdc42-mediated microspike formation. Although ZCL278 displayed the most striking inhibitory effects on microspike formation among the 30 compounds tested, four other promising compounds identified from the virtual screening showed similar properties. The chemical structures of these four compounds, along with six other ZCL compounds, are described in *SI Materials and Methods* (Fig. S2).

In our *in silico* screening model, the Cdc42–ITSN interaction interface defines a binding pocket of 16 residues in Cdc42. We aligned the sequences of Cdc42 (P60953; from UniProt; www.uniprot.org/uniprot/), Rac1 (P63000), and RhoA (P61586; Fig. S3). One of the 16 residues is different between Cdc42 and Rac1 [Phe56 (Cdc42)/Trp56 (Rac1)], whereas three residues are different between Cdc42 and RhoA [Asp38 (Cdc42)/Glu40 (RhoA), Phe56/Trp58, Gln74/Asp76]. The determinant for the selectivity of these Rho GTPases toward their GEFs is Phe56 (Cdc42)/Trp56 (Rac1)/Trp58 (RhoA). We thus further performed studies to compare ZCL278 with Y-27632, a RhoA/Rho kinase inhibitor (19, 20), under the condition that RhoA is activated (Fig. 2*B*, *Left*). We also performed studies to compare ZCL278 with NSC23766, a Rac1-selective inhibitor (21), under the condition that Rac1 is activated (Fig. 2*B*, *Right*). These results demonstrated that ZCL278 inhibits Cdc42-mediated (Fig. 2*A*), but not RhoA- or Rac1-mediated, phenotypes (Fig. 2*B*).

ZCL278 Inhibits Cdc42 Activity. As ZCL278 showed direct binding to Cdc42 and displayed most inhibitory effects in a morphological assay of Cdc42 function, we analyzed its activity at a biochemical level. First, Cdc42 activation was investigated in human metastatic prostate cancer PC-3 cells that were treated with the Cdc42 activator or 50 μM ZCL278 for 5, 10, and 15 min. Serine 71 phosphorylation is known to negatively regulate Rac/Cdc42 activity (22), and therefore an increase in phospho-Rac/Cdc42 expression is indicative of a decrease in active (i.e., GTP-bound) Rac/Cdc42. As depicted in Fig. 2*C*, activation of Cdc42 shows an expected decrease in phospho-Rac/Cdc42. However, the application of ZCL278 resulted in a time-dependent increase in Rac/Cdc42 phosphorylation.

Wiskott–Aldrich syndrome protein (WASP) is a downstream effector of Cdc42 activation (6). Tyrosine phosphorylation of WASP is linked to rapid Cdc42 degradation following its activation

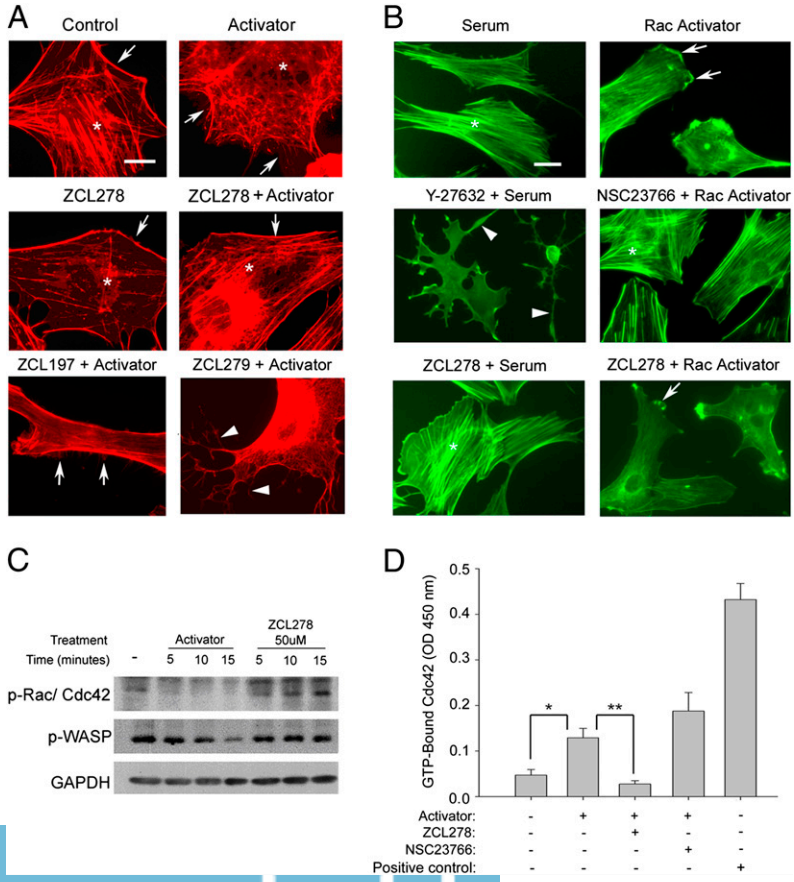

Fig. 2. Characterization of ZCL278 functions. (*A*) ZCL278, but not ZCL197 or ZCL279, inhibits Cdc42-mediated microspike formation. Serum-starved Swiss 3T3 cells were treated with or without Cdc42 ligands identified by the high-throughput *in silico* screening. DMSO was used as a control, and 1 U/mL Cdc42 activator was applied to stimulate Cdc42. ZCL278 (50 μM), ZCL197, or ZCL279 was applied for 15 min without activation of Cdc42 or for 1 h and then stimulated with the Cdc42 activator for 2 min. Following treatments, cells were fixed and stained with rhodamine–phalloidin to label filamentous actin. Arrows point to the cell periphery, where microspikes may be seen. Asterisks indicate the subcellular locations that normally show stress fiber distribution. (Scale bar: 5 μm.) (*B*) ZCL278 does not induce RhoA inhibition-mediated branching of cellular processes, nor does it suppress Rac1-mediated lamellipodia formation. Asterisks indicate stress fiber distribution, arrows point to lamellipodia, and arrowheads point to branched cellular processes. (Scale bar: 5 μM.) (*C*) ZCL278 inhibits endogenous Rac/Cdc42 activities. Serum-starved PC-3 cells were treated with the Cdc42 activator at 1 U/mL or 50 μM ZCL278 for the indicated time points. Cell lysates were subjected to Western blot analysis with the following antibodies: phospho-Rac1/cdc42 (*Top*), phospho-WASP (*Middle*), and GAPDH (*Bottom*). (*D*) ZCL278, but not NSC23766, inhibits stimulated Cdc42 activity. Serum-starved Swiss 3T3 cells were incubated for 1 h with 50 μM ZCL278 or 10 μM NSC23766 and then stimulated for 2 min with a Cdc42 activator at 1 U/mL. Cell lysates were then subjected to a colorimetric G-LISA assay to measure GTP-bound Cdc42. A constitutively active Cdc42 was used as positive control. Negative controls included buffer-only controls as well as untreated cellular lysates. Results shown are averaged from three independent experiments ($n = 3$ per group) ± SE (**$P < 0.01$, *$P < 0.05$).

(23, 24). As shown in Fig. 2*C*, the Cdc42 activator leads to a decreased expression of phospho-WASP by 15 min whereas ZCL278 does not suppress phospho-WASP activity. Thus, ZCL278 inhibits Rac/Cdc42 phosphorylation in a time-dependent manner and maintains tyrosine phosphorylation of WASP.

Serine 71 phosphorylation can occur on Rac and Cdc42. To directly assess specific Cdc42 activation and inactivation, we used a G-LISA, an ELISA-based assay that allows a quantitative determination of the levels of GTP-bound (i.e., active) Cdc42 in cellular lysates. Serum-starved Swiss 3T3 fibroblasts were incubated for 1 h with 50 μM ZCL278 or 10 μM NSC23766 (Rac inhibitor), followed by 2 min of stimulation with 1 U/mL Cdc42 activator. This analysis revealed a significant increase (70%) in GTP-bound Cdc42 in cells treated with the activator compared with control (i.e., untreated) cells (Fig. 2*D*). Cells treated with ZCL278 showed a dramatic (nearly 80%) decrease in GTP-Cdc42 content compared with cells treated solely with the activator. Finally, we analyzed the ability of NSC23766 to determine if it cross-inhibits Cdc42 activation. NSC23766 was developed in a similar manner as ZCL278; however, it is specific to Rac and should therefore act as an additional negative control in this assay (21). As expected, NSC23766 does not reduce GTP-Cdc42 content (Fig. 2*D*). These data establish that ZCL278 inhibits Cdc42 in two different cell types.

ZCL278, but Not NSC23766, Disrupts Perinuclear Distribution of Active Cdc42. To confirm the ability of ZCL278 to selectively inhibit Cdc42 activation at the cellular level, serum-starved Swiss 3T3 cells were treated with 50 μM ZCL278 or 10 μM NSC23766 and were subsequently stimulated for 2 min with the Cdc42 activator (Fig. 3). Cells were probed with a mouse monoclonal antibody against active (i.e., GTP-bound) Cdc42 (Fig. 3*A*). Nuclei were visualized by Hoechst staining. Control fibroblasts showed an organized perinuclear distribution of active Cdc42 (Fig. 3*A*). Cdc42 activation increased this distribution in the perinuclear region as well as in the nucleus (Fig. 3*A*), consistent with the established

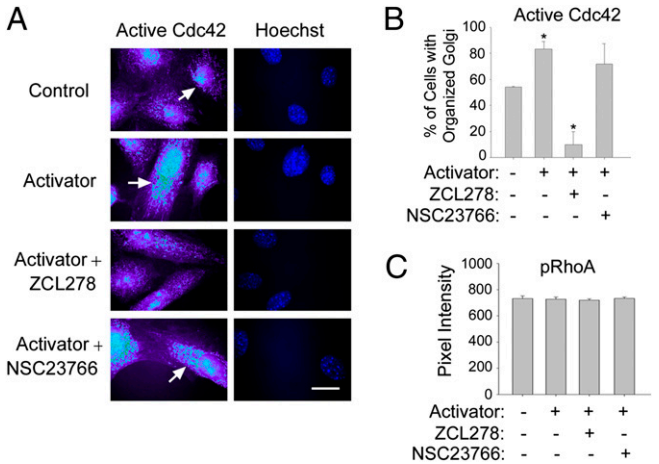

Fig. 3. Immunofluorescence light microscopy of active Cdc42 and phosphorylated RhoA. Serum-starved Swiss 3T3 cells were treated with DMSO as control, Cdc42 activator, 50 μM ZCL278, or 10 μM NSC23766. Treatments with ZCL278 or NSC23766 were followed by stimulation for 2 min with a Cdc42 activator at 1 U/mL To determine if ZCL278 selectively inhibits Cdc42 but not RhoA activity, cells were probed with an active Cdc42 (*A* and *B*) or phosphorylated RhoA (*C*) antibodies. Arrows mark perinuclear Golgi–endoplasmic reticulum (ER) network. Nuclei were visualized by Hoechst staining. (Scale bar: 15 μm.) (*B*) Active Cdc42 associated with organized perinuclear Golgi–ER network was quantified. Organized Golgi–ER was quantified in five randomly selected regions of cells in each treatment group using the pseudocolor setting (*$P < 0.05$). (*C*) Pixel intensity of phospho-RhoA in cells after treatments with activator, ZCL278, or NSC23766 was quantified. Results reflect the averaged intensity generated at five random points in five independent cells ($n = 5$ per group) ± SE (*$P < 0.03$).

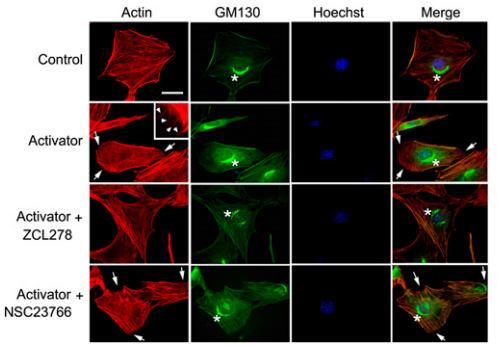

Fig. 4. ZCL278 disrupts GM130 docked Golgi organization. Serum-starved Swiss 3T3 cells were treated with DMSO as control, a Cdc42 activator, ZCL278, or NSC23766. Following the treatment, cells were stained by rhodamine–phalloidin (red), anti-GM130 (green), and Hoechst (blue). Arrows point to the cell edges, where microspikes can be seen (red). (*Inset*) High-magnification image of cells treated with the Cdc42 activator; arrowheads point to microspikes. Asterisks (green) point to the Golgi structure immunolabeled by anti-GM130. Cdc42 activation led to increased microspikes, as expected [activator indicated by arrows and arrowheads (*Inset*)], and intense perinuclear GM130 immunoreactivity (activator indicated by asterisk). Cells treated with ZCL278 showed fewer microspikes (ZCL278; red). GM130 immunoreactivity is clearly reduced and distributed to both sides of the nucleus (ZCL278; green asterisk). Rac inhibitor NSC23766 did not significantly alter microspike formation (NSC23766; red arrows) and GM130 expression or distribution (NSC23766; green asterisk). (Scale bar: 10 μm.)

roles of Cdc42 in Golgi-based protein trafficking (25). ZCL278 clearly disrupted this organization and reduced immunoreactivity of anti-active Cdc42 whereas NSC23766 did not have the same effects (see also the quantification of the percentage of cells showing organized Golgi-like distribution in Fig. 3*B*). Additionally, application of the Cdc42 activator, ZCL278, or NSC23766 did not elicit significant changes in phospho-RhoA immunoreactivity (Fig. 3*C*). These results again indicate that ZCL278 selectively inhibits Cdc42.

ZCL278, but Not NSC23766, Disrupts GM130 Docked Golgi Organization. To determine whether the ZCL278-induced disruption of perinuclear distribution of active Cdc42 reflected its effects on Golgi organization, we examined GM130, a peripheral cytoplasmic protein that is tightly bound to Golgi membranes and helps to maintain *cis*-Golgi structures (26, 27). Control, serum-starved Swiss 3T3 cells showed well-developed stress fibers (Fig. 4, red) and GM130 immunoreactivity polarizing to one side of the nucleus (Fig. 4, green asterisk). Treatment with the Cdc42 activator led to increased microspikes, as expected [Fig. 4, red arrows, arrowheads (*Inset*)], and intense perinuclear GM130 immunoreactivity (Fig. 4, green asterisk). As depicted in Fig. 4 (also see Fig. 2*A*), ZCL278-treated cells show not only fewer microspikes but also a clear reduction of GM130 immunoreactivity, as well as its dissipation to both sides of the nucleus (Fig. 4, green asterisk). Rac inhibitor NSC23766 did not significantly alter GM130 expression or distribution (Fig. 4, green asterisk). These results not only further confirm ZCL278 as a specific Cdc42 inhibitor, but also demonstrate the importance of Cdc42 in Golgi organization and protein trafficking.

ZCL278 Impedes Wound Healing Without Disruption of Cell Viability. Filopodia are dynamic structures that aid cells in pathfinding and migration (28, 29), and are largely controlled by Cdc42 activity (30). In a metastatic line of human prostate cancer cells (PC-3), we used a wound healing assay to elucidate the effects of ZCL278 on cellular migration. Quiescent PC-3 cells were wounded with a sterile pipette tip and treated with or without the Cdc42 activator, ZCL278, or the Rac inhibitor NSC23766 for 24 h. As shown in Fig. 5*A* and quantified in Fig. 5*B*, Cdc42 activation resulted in a significant increase (59%) in wound healing ability in comparison with controls (41%). Application of 50 μM and 5 μM ZCL278

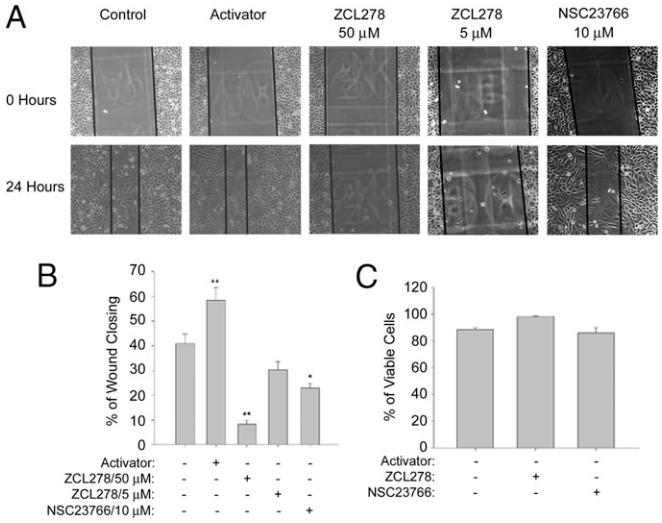

Fig. 5. ZCL278 impedes cellular migration without disruption of cell viability. (*A*) Serum-starved PC-3 cells were grown to confluent monolayers, wounded using a sterile pipette tip, and incubated for 24 h with a Cdc42 activator at 1 U/mL, 50 μM ZCL278, 5 μM ZCL278, or 10 μM NSC23766. The distance of migration was then analyzed by phase-contrast microscopy and MetaMorph software. Black lines indicate the leading edge of the wound. (*B*) Wound healing was quantified at 0 and 24 h by measuring the shortest distance between the edges of the scratch. Columns represent the wound healing as a percentage of the original wound distance. Results shown are averaged from three independent experiments ($n = 3$ per group) ± SE (**$P < 0.01$, *$P < 0.05$). (*C*) Serum-starved PC-3 cells were incubated for 24 h with 50 μM ZCL278 or 10 μM NSC23766. Cell viability was determined by using a Countess Automated Cell Counter (Invitrogen) combined with trypan blue dye staining of cells.

inhibited PC-3 migration into the wound area. However, wound closure was less pronounced at 50 μM (8%) than 5 μM (30%) concentrations. Cellular migration was also significantly reduced with NSC23766 treatment. This result is to be expected, as Rac regulates the formation of lamellipodia, which are well-described motile structures (31). These data, which are in agreement with our biochemical analysis, suggest that ZCL278 is not only a selective inhibitor of Cdc42 activation but also a potent suppressor of Cdc42-dependent cell motility.

To ensure that decreases in cellular migration seen with ZCL278 treatment was a result of Cdc42 inhibition (or Rac inhibition when treated with NSC23766) rather than cell death, we tested cell viability by using the trypan blue dye exclusion assay. PC-3 cells were arrested in G_0, and then 50 μM ZCL278 or 10 μM NSC23766 was applied for 24 h. Fig. 5*C* demonstrates that there was no difference in viability between treated and nontreated (i.e., control) cells. Therefore, we conclude that the differences seen in migratory ability is a result of ZCL278-mediated Cdc42 inhibition or NSC23766-mediated Rac inhibition and not cell death.

ZCL278 Inhibits Neuronal Branching and Growth Cone Dynamics. Cdc42 plays a crucial role in the establishment of neuronal morphogenesis (13). Cdc42's absence in neurons resulted in a significantly reduced number of neurites and severely disrupted filopodia function (32). Therefore, we tested the ability of ZCL278 to inhibit neuronal branching in primary neonatal cortical neurons.

At 5 d cultured in vitro, cortical neurons extended neurites with multiple branches (Fig. 6*A*, control). ZCL278 (50 μM) was applied for 5 and 10 min, whereas DMSO-treated neurons were maintained as negative controls. As demonstrated in Fig. 6*A*, neuronal branching was suppressed in ZCL278-treated neurons over the time course in comparison with the highly branched neurites of control cells. Quantitative measurements found the branch number to be significantly reduced in ZCL278-treated neurons (Fig. 6*B*).

Cdc42 is also widely known to control filopodia and microspikes at the leading edge of migrating growth cones (33). Time-lapse video light microscopy shows a control cortical neuron with multiple microspikes or filopodia extended from the growth cone (Fig. 6*C*). However, ZCL278 treatments resulted in rapid retraction of filopodia within 4 min (Fig. 6*C*). Thus, these studies further support ZCL278 as an effective small-molecule inhibitor of Cdc42-mediated neuronal branching and growth cone motility.

Discussion

Signaling through the Rho GTPase pathway allows cells to accomplish a myriad of cellular tasks, including membrane trafficking, cell cycle control, and the regulation of cytoskeletal organization, which strongly influence cell morphology, motility, and cell fate (34–36). Currently, many pathological conditions have been attributed to Rho GTPase dysfunction or deregulation, making them prime candidates for pharmaceutical intervention (5, 37).

The available small molecule modulators of Rho GTPases have facilitated the exploitation of this important family of proteins. Notably, fasudil and Y-27632 are well-established and potent inhibitors of Rho kinase/$p160^{ROCK}$, one of the main downstream effectors of RhoA (19, 20). Recent development of NSC23766 targeting Rac1–GEF interaction filled a gap for studies on Rac as a selective Rac1 inhibitor (21). However, there are few choices for effective small-molecule inhibitors selective for Cdc42. Secramine, an analogue of natural product galanthamine, was discovered recently by its ability to inhibit Cdc42-dependent Golgi to membrane transport through RhoGDI1 (38). Unlike the widely used Y-27632 ($N = 1{,}903$ publications) or NSC23766 ($N = 115$ publications), secramine availability is very limited, and few studies can be found in literature today ($N = 9$ publications). Cdc42 deregulation has been linked to various aspects of tumorigenesis, including transformation and metastasis (3, 39). Additionally, neuronal development and maintenance relies heavily on appropriate Cdc42 activity (8). Given the urgent need to discover an effective tool for Cdc42 study, we undertook a similar strategy in the discovery of NSC23766 and identified potential Cdc42 inhibitors by screening more than 197,000 small molecules coupled with biochemical and cell-based verifications. Among the 30 potential

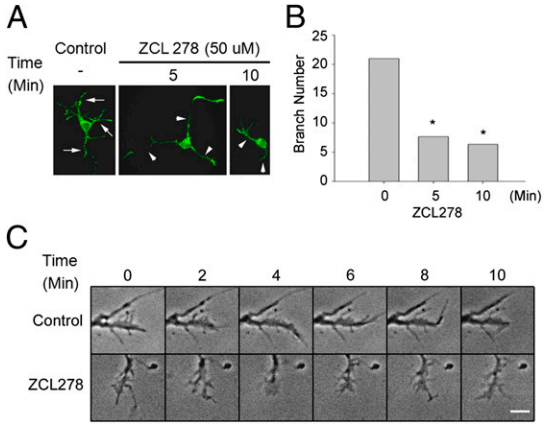

Fig. 6. ZCL278 inhibits neuronal branching and growth cone motility. Primary cortical neurons from postnatal day 1 mouse pups were cultured on poly-L-lysine–coated coverslips. (*A*) Neurons were treated at 5 d in vitro with DMSO (control) or 50 μM of ZCL278 for 5 and 10 min. Neurons were then fixed, and actin-based structures were identified with rhodamine–phalloidin labeling. Whereas control neurons showed multiple branches (arrows), ZCL278 treatment reduced the branch numbers (arrowheads). (*B*) The number of branches was counted on neurons treated with ZCL278. Results shown are averaged from three independent experiments ($n = 3$ per group) ± SE (*$P < 0.01$). (*C*) Time-lapse imaging of cortical neuronal growth cone motility. Whereas the control neuron maintains multiple microspikes or filopodia, ZCL278 treatment led to rapid retraction of microspikes or filopodia. (Scale bar: 1 μm.)

BIOCHEMISTRY

leads that interfered with fibroblastic cell morphology related to Cdc42 function, ZCL278 emerged as the most effective and selective compound. ZCL278 synthesis involves few steps and is cell-permeable, and is therefore quite amenable to further exploitation as a pharmaceutical lead. In this study, we provide evidence for the characterization of an effective Cdc42 small-molecule inhibitor, which specifically and directly targets the binding site of its GEF, ITSN. This is yet another example of identification of a small-molecule modulator of biologically significant signaling pathways based on computer-assisted screening (21, 40).

Several studies have previously demonstrated the importance of Cdc42 activation for epithelial-to-mesenchymal transition and resultant cellular movement that is necessary for cancer cell invasion (11, 12). By using a wound-healing assay, we showed that treatment with a Cdc42 activator is capable of enhancing wound closure in comparison with nontreated cells, bolstering evidence for Cdc42's ability to enhance the metastatic activity of cancer cells. Significantly, ZCL278 was able to inhibit the migratory ability of PC-3 cells in a concentration-dependent manner. Furthermore, ZCL278 is not cytotoxic to cells, and cell death is not the reason for the significant reduction in migration. Our studies raised an exciting possibility that ZCL278 can potentially be used for further investigation of its ability to inhibit cancer cell invasion and metastasis in vivo.

Our studies on primary cortical neurons also support the role of Cdc42 in neuronal development. As elegantly demonstrated by Garvalov et al. in 2007 (13), brain and neuronal development are severely disrupted in Cdc42-deficient mice. These mice exhibit a range of brain abnormalities, including reduced axonal tracts, whereas neurons displayed a decrease in filopodial dynamics, increased growth cone size, and suppressed axon generation. Application of Cdc42 inhibitor ZCL278 to primary neurons reduced the number of branches formed and impeded growth cone dynamics. This is consistent with the notion that axon and dendrite motility is largely an actin-based process that is highly regulated by Cdc42 (41). Thus, ZCL278 is a small-molecule inhibitor of Cdc42–ITSN interaction, and provides a powerful tool for further elucidation of Cdc42 function in human diseases, including cancer and neurologic diseases.

Materials and Methods

Virtual Screening, Compound Synthesis, Affinity Measurements, and Other Biochemical and Cell-based Assays. The Glide program (Schrodinger) was used to screen the Specs database consisting of 197,000 compounds. The fluorescence of tryptophan was measured as described by Zhou et al (42). The computation methods, compound synthesis, determination of in vitro ZCL278-Cdc42 binding affinity by fluorescence titration and SPR, determination of protein distribution and expression, are detailed in *SI Materials and Methods*. G-LISA, p50RhoGAP or Cdc42GAP experiments, wound healing assay as well as primary neurons and time-lapse imaging are also detailed in *SI Materials and Methods*.

ACKNOWLEDGMENTS. We thank Christi Boykin, Zhe Lu, and Jiao Zhang for technical assistance. This work was supported in part by National Cancer Institute Grants CA111891 and CA165202 (to Q.L.), the Harriet and John Wooten Laboratory for Alzheimer's Disease Research (Q.L.), National Natural Science Foundation of China Grant 81222042 (to H.Z.), Ministry of Science and Technology of China Grants 2009CB918404 and 2012CB518001 (to H.Z.), and the E-Institutes of Shanghai Universities Chemical Biology Division (H.Z.).

1. Johnson D-I, Pringle J-R (1990) Molecular characterization of CDC42, a Saccharomyces cerevisiae gene involved in the development of cell polarity. *J Cell Biol* 111(1):143–152.
2. Cerione R-A (2004) Cdc42: New roads to travel. *Trends Cell Biol* 14(3):127–132.
3. Stengel K, Zheng Y (2011) Cdc42 in oncogenic transformation, invasion, and tumorigenesis. *Cell Signal* 23(9):1415–1423.
4. Sinha S, Yang W (2008) Cellular signaling for activation of Rho GTPase Cdc42. *Cell Signal* 20(11):1927–1934.
5. Lu Q, Longo F-M, Zhou H, Massa S-M, Chen Y-H (2009) Signaling through Rho GTPase pathway as viable drug target. *Curr Med Chem* 16(11):1355–1365.
6. Ridley A-J (2006) Rho GTPases and actin dynamics in membrane protrusions and vesicle trafficking. *Trends Cell Biol* 16(10):522–529.
7. Ellenbroek S-I, Collard J-G (2007) Rho GTPases: Functions and association with cancer. *Clin Exp Metastasis* 24(8):657–672.
8. Auer M, Hausott B, Klimaschewski L (2011) Rho GTPases as regulators of morphological neuroplasticity. *Ann Anat* 193(4):259–266.
9. Rihet S, et al. (2001) Mutation status of genes encoding RhoA, Rac1, and Cdc42 GTPases in a panel of invasive human colorectal and breast tumors. *J Cancer Res Clin Oncol* 127(12):733–738.
10. Lin R, Cerione R-A, Manor D (1999) Specific contributions of the small GTPases Rho, Rac, and Cdc42 to Dbl transformation. *J Biol Chem* 274(33):23633–23641.
11. Chen L, et al. (2010) CHD1L promotes hepatocellular carcinoma progression and metastasis in mice and is associated with these processes in human patients. *J Clin Invest* 120(4):1178–1191.
12. Johnson E, et al. (2010) HER2/ErbB2-induced breast cancer cell migration and invasion require p120 catenin activation of Rac1 and Cdc42. *J Biol Chem* 285(38):29491–29501.
13. Garvalov B-K, et al. (2007) Cdc42 regulates cofilin during the establishment of neuronal polarity. *J Neurosci* 27(48):13117–13129.
14. Ahmad K-F, Lim W-A (2010) The minimal autoinhibited unit of the guanine nucleotide exchange factor intersectin. *PLoS ONE* 5(6):e11291.
15. Goreshnik I, Maly D-J (2010) A small molecule-regulated guanine nucleotide exchange factor. *J Am Chem Soc* 132(3):938–940.
16. Snyder J-T, et al. (2002) Structural basis for the selective activation of Rho GTPases by Dbl exchange factors. *Nat Struct Biol* 9(6):468–475.
17. Kozma R, Ahmed S, Best A, Lim L (1995) The Ras-related protein Cdc42Hs and bradykinin promote formation of peripheral actin microspikes and filopodia in Swiss 3T3 fibroblasts. *Mol Cell Biol* 15(4):1942–1952.
18. Nobes C-D, Hall A (1995) Rho, rac and cdc42 GTPases: Regulators of actin structures, cell adhesion and motility. *Biochem Soc Trans* 23(3):456–459.
19. Uehata M, et al. (1997) Calcium sensitization of smooth muscle mediated by a Rho-associated protein kinase in hypertension. *Nature* 389(6654):990–994.
20. Suzuki Y, et al. (1999) Agonist-induced regulation of myosin phosphatase activity in human platelets through activation of Rho-kinase. *Blood* 93(10):3408–3417.
21. Gao Y, Dickerson J-B, Guo F, Zheng J, Zheng Y (2004) Rational design and characterization of a Rac GTPase-specific small molecule inhibitor. *Proc Natl Acad Sci USA* 101(20):7618–7623.
22. Kwon T, Kwon D-Y, Chun J, Kim J-H, Kang S-S (2000) Akt protein kinase inhibits Rac1-GTP binding through phosphorylation at serine 71 of Rac1. *J Biol Chem* 275(1):423–428.
23. Torres E, Rosen M-K (2003) Contingent phosphorylation/dephosphorylation provides a mechanism of molecular memory in WASP. *Mol Cell* 11(5):1215–1227.
24. Torres E, Rosen M-K (2006) Protein-tyrosine kinase and GTPase signals cooperate to phosphorylate and activate Wiskott-Aldrich syndrome protein (WASP)/neuronal WASP. *J Biol Chem* 281(6):3513–3520.
25. Harris K-P, Tepass U (2010) Cdc42 and vesicle trafficking in polarized cells. *Traffic* 11(10):1272–1279.
26. Erickson J-W, Zhang C, Kahn R-A, Evans T, Cerione R-A (1996) Mammalian Cdc42 is a brefeldin A-sensitive component of the Golgi apparatus. *J Biol Chem* 271(43):26850–26854.
27. Nakamura N, et al. (1995) Characterization of a cis-Golgi matrix protein, GM130. *J Cell Biol* 131(6 Pt 2):1715–1726.
28. Gupton S-L, Gertler F-B (2007) Filopodia: The fingers that do the walking. *Sci STKE* 2007(400):re5.
29. Nemethova M, Auinger S, Small J-V (2008) Building the actin cytoskeleton: Filopodia contribute to the construction of contractile bundles in the lamella. *J Cell Biol* 180(6):1233–1244.
30. Yang L, Wang L, Zheng Y (2006) Gene targeting of Cdc42 and Cdc42GAP affirms the critical involvement of Cdc42 in filopodia induction, directed migration, and proliferation in primary mouse embryonic fibroblasts. *Mol Biol Cell* 17(11):4675–4685.
31. Ridley A-J, Hall A (1992) The small GTP-binding protein rho regulates the assembly of focal adhesions and actin stress fibers in response to growth factors. *Cell* 70(3):389–399.
32. Govek E-E, Newey S-E, Van Aelst L (2005) The role of the Rho GTPases in neuronal development. *Genes Dev* 19(1):1–49.
33. Brown M-D, Cornejo B-J, Kuhn T-B, Bamburg J-R (2000) Cdc42 stimulates neurite outgrowth and formation of growth cone filopodia and lamellipodia. *J Neurobiol* 43(4):352–364.
34. Hall A (1998) Rho GTPases and the actin cytoskeleton. *Science* 279(5350):509–514.
35. Jaffe A-B, Hall A (2005) Rho GTPases: Biochemistry and biology. *Annu Rev Cell Dev Biol* 21:247–269.
36. Wennerberg K, Der C-J (2004) Rho-family GTPases: It's not only Rac and Rho (and I like it). *J Cell Sci* 117(Pt 8):1301–1312.
37. Fritz G, Kaina B (2006) Rho GTPases: Promising cellular targets for novel anticancer drugs. *Curr Cancer Drug Targets* 6(1):1–14.
38. Pelish H-E, et al. (2006) Secramine inhibits Cdc42-dependent functions in cells and Cdc42 activation in vitro. *Nat Chem Biol* 2(1):39–46.
39. Boettner B, Van Aelst L (2002) The role of Rho GTPases in disease development. *Gene* 286(2):155–174.
40. Massa S-M, Xie Y, Longo F-M (2002) Alzheimer's therapeutics: Neurotrophin small molecule mimetics. *J Mol Neurosci* 19(1-2):107–111.
41. Watabe-Uchida M, Govek E-E, Van Aelst L (2006) Regulators of Rho GTPases in neuronal development. *J Neurosci* 26(42):10633–10635.
42. Zhou H, et al. (2006) Structure-activity studies on a library of potent calix[4]arene-based PDGF antagonists that inhibit PDGF-stimulated PDGFR tyrosine phosphorylation. *Org Biomol Chem* 4(12):2376–2386.